Research Article DOI: Open Access

Influence of Precipitation Variability on Porewater Pressure and Surface Layer Failures in Naturally Undulating Slopes at Nau Kilo, Narayanghat–Mugling Road, Central Nepal

Samyog Khanal[1]* and Ranjan Kumar Dahal[2]

[1]Kajaria Ramesh Tiles Ltd., Team Venture Building, 3rd floor, Sinamangal, Kathmandu, Nepal
[2]Central Department of Geology, Tribhuvan University, Kathmandu, Nepal

(*Corresponding E-mail: Samyogkhanal2017@gmail.com)

Received: July 15, 2024, Accepted on November 05, 2024

Abstract: This study investigates the role of porewater pressure variations in slope failures within naturally undulated hill slopes characterized by topographic hollows. A representative slope with a distinct hollow and six rainfall-induced failures recorded between 2001 and 2023 was selected for detailed analysis. Seepage and slope stability modeling were conducted in GeoStudio using the July 31, 2003, precipitation event, with simulations incorporating 24-hour maximum rainfall data corresponding to 5, 10, 25, 50, and 100-year return periods. These events were normalized using 6-minute interval rainfall data, and potential seepage face boundary conditions were applied. The results demonstrated a threshold relationship between hollow area and maximum porewater pressure, indicating that larger hollows generate higher porewater pressures under extreme rainfall. Specifically, a hollow of 100 m^2 was found to develop a maximum porewater pressure of 6.94 kPa. The findings highlight that topographic hollows act as hydrological convergence zones, increasing subsurface saturation and instability during intense rainfall events. The developed threshold relationship offers a predictive framework for assessing slope failure susceptibility in similar geomorphic settings, contributing to more effective hazard assessment and early warning systems.

Keywords: ***Hillslope Hydrology, Threshold for shallow failure, Porewater pressure.***

Introduction

Seepage and slope stability modeling is one of the crucial factors in the analysis of the rainfall-induced slope failure present in the naturally undulated slope. The landscape present in the concave depression that collects water and consists of steep slopes, which can trigger slope failure during heavy rainfall events is called a naturally undulated slope. It is important to consider the soil characteristics, moisture content, geometry of the slope, and forces developed by rainfall events for the slope stability analysis. Setyawan et al. (2021). The intense rainfall reduces the shear strength of the soil by gradually increasing pore water pressure, which leads to the instability of the slope Setyawan et al. (2021). Thus, the seepage and slope stability model are applied in naturally undulated slopes to recognize possible processes leading to slope failure and to provide proper guidance leading to the mitigation measures Acharya et al. (2016). Seepage modeling is the process of examining the flow of moisture in and out of the soil and dealing with the evolution of pore water pressure within the soil. Analytical methods, numerical methods, and physical methods are some widely used methods to model seepage in the slope. Finite element analysis and finite difference methods are examples of numerical methods that are complex and need more pragmatic geometrics and boundary conditions. Constructed scaled model of the slope is simulated through the flow of water in the physical models Khan and Wang (2021). In insertion to seepage modeling, slope stability analysis plays an important role in griping the prospective for slope failure in naturally undulated slopes Setyawan et al. (2021). The limit equilibrium analysis, finite element analysis, and numerical methods are some types of modeling techniques widely used for slope stability. The factor of safety against failure is calculated by processing the different forces acting on the slope is commonly used in the limit equilibrium analysis in geotechnical engineering Khan and Wang (2021). The slope is classified into the small parts and analyzing it with the forces acting on each element to obtain the factor of safety against failure is done for the finite elements methods Khan and Wang (2021). The infiltration rate and the pore water pressure dealing out within the slope is generally influenced by rainfall intensity, duration and distribution of rainfall, so it important to model the rainfall infiltration and development of pore water pressure in the slope face Sun et al. (2022). In general, unsaturated flow models are widely used to model the simulation of the infiltration of the rainfall into soil for the development of the pore water pressure within the slope face Acharya et al. (2016). Shallow landslide and debris flows can be generated by the enormous and short rainfall in the soil with high permeability as explained by Campbell (1975), while common rainfall dealing with an extended period leads to deep as well as shallow landslides in the region's soil having low permeability was explained by Cardinali et al., (2006) in his study. The intensity and the duration of rainfall along with the distribution of permeability of soils play an important role in describing the type of landslide described by Dahal and Hasegawa

(2008), Pasuto and Silvano (1998). The characteristics and pattern of rainfall along with their regional area plays an important role in the landslide threshold value from one place to another with the combination of factors like lithology of the area, climate of the area, geological past histories, soil characteristics and geometry of the slope was explicate by Crosta (1998), Van Asch et al. (1999) and its relation with time was explained by Crozier (1999). When there was an excellent number of databases available in connection with the rainfall events and add the landslide the threshold for landslide. occurring event were predicted by the help of a statistical model Dahal et al. (2008).

The rainfall leads to the rainfall infiltration to develop the porewater pressure was analyzed with the help of a hydrological model as explained by Frattini et al. (2009) in his work. The development of the positive porewater pressure leads to the deep-seated failure by decreasing metric suction leading to the slope failure has been noticed by the Guzzetti et al. (2004). Topographical flow routing based on the hydrological model in saturated and unsaturated conditions was used to simulate the failure mechanism. TOPMODEL Beven and Kirkby (1979), HILLFLOW Bronstert (1994), SHALSTAB Dietrich et al. (1998), and SINMAP Pack et al. (1999) were some examples of hydrological slope stability analysis model widely used. By the help of SEEP/W and SLOPE/W of GeoStudio (2018) was hydrological slope stability model was in use in modern days.

The naturally undulated slopes were also called topographic hollow. The convex topography with thick colluvium deposited and tends to be deposited with much infiltrated water as a result of extreme rainfall events was called naturally undulated slopes. The have capacity to evacuate slowly compared to the ridges as explained by Dunne (1978). Deposit from existing vegetation, throw away of material around the scar, gradient of slope with its type, action of wind, creeped materials, and presence of organic material plays an important role of depositions of material in the naturally undulated soles Dietrich and Dunne (1978). The liquefaction was the one of the most effects observed in the naturally undulated slopes by Sassa (1986). Based on the mode of development and depositions they were classified as A type and B type by the Tsukamoto and Minematsu (1987). Geotechnical parameters of soils, gradient and aspect of slope, strength of vegetation root, thickness of he deposited soil plays an important role in the failure of the naturally undulated slopes Sidle (1987). After a certain period of time of the deposition, the slope failure can occur leading to the deposition of new slope materials. That was the reason why the undulated slopes were believed to be in vogue and soon failure may occur Dietrich (1987). The small-scale landslides were generally the most prominent features in the naturally undulated slopes Yatabe et al. (2016). Numerous numbers of computer-based software have been created for the examination and determination of the factor of safety (FOS) of the slope. The detailed field observation data with the geometry of the was easily simulated and modeled with the help of different software. "SHIVA" was the software developed by Wagner et al. (1990) that can be used to create rock and soil hazard maps in the research field of Nepal. "CLARA" was used by Marquez (2004) used for the three-dimensional slope stability analysis. Rocscience developed da comprehensive 2D slope stability software "SLIDE" for the study of the groundwater seepage and stability of the dams was used by Kvalstad et al. (2005). FLAC (Fast Lagrangian Analysis of Continua) used in the field of geotechnical, civil and mining operations to model the groundwater seepage and its vulnerability on the slopes Pradhan (2014). "GeoStudio 2018" put forward Seep/W and slope for seepage and slope stability analysis was used by Acharya (2016). "PLAXIS" was famous software for the geotechnical study of the slopes and its stability analysis used by Jacob et al. (2018).

Study Area

Location and Geology of the area

The study area is located in the Bagmati Province, Chitwan District, Ichchhakamana Rural Municipality near the Koyalghari area Figure 1. The study area can be accessed through road by major highway of Nepal. The study area can be approached from Kathmandu through the Tribhuvan Rajpath and the Narayanghad Muglin highway. The area of interest is also accessed by flight or through airway taking flights up to Bharatpur Airport and up to the research area. Geologically, the research area lies in the Autochthonous Unit of the Lesser Himalaya, mainly in the Labdi Khola Member of the Nourpul Formation.

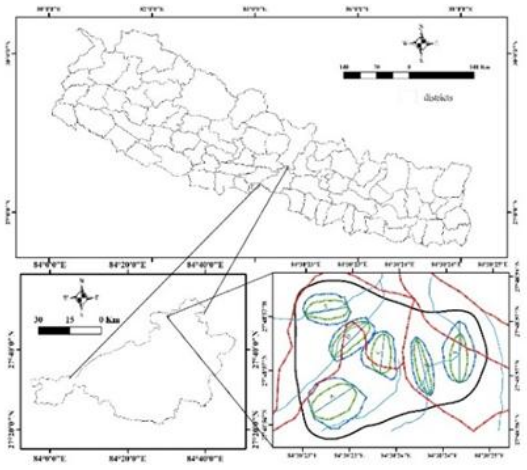

Figure 1, Location map of the study area.

The outcrop comprises interbedded phyllite and quartzite. The phyllite is reddish-brown to green on weathered surfaces and dark grey to light grey on fresh surfaces. It is thinly foliated with an average foliation spacing of approximately 8 cm and exhibits slight to moderate weathering. The quartzite beds are fine- to medium-grained, dark grey, and display slight to moderate weathering. Bedding thickness varies from thinly to thickly bedded, ranging from 12 to 22 cm. The

overall lithological contact is conformable, indicating a well-developed interbedding relationship between the phyllite and quartzite units. The colluvium and alluvial deposited material are also observed in the study area Figure 2.

Rainfall in the study area

Rainfall data from 2001 to 2023 A.D. were analyzed to assess precipitation patterns in the study area. The highest recorded 24-hour rainfall was 446.30 mm on July 31, 2003. The study area, situated within a subtropical climate zone, experiences a pronounced monsoon season extending from June to September, during which the majority of annual precipitation occurs. The climate is characterized by unevenly distributed rainfall, as evidenced by meteorological records. The mean annual rainfall over the study period varies considerably, with the maximum total annual precipitation reaching 3,164.70 mm in 2003. That same year also recorded the highest monsoonal rainfall, amounting to 2,598.40 mm. Temperature in the region ranges from a minimum annual average of 23.6°c to a maximum of 35°c. These climatic conditions contribute significantly to slope hydrology and potential instability, especially during peak monsoonal events.

Figure 2, Geological map of the study area.

Materials and Methods

Fieldwork

The field investigation was done to gather the length/width of slope failure zones, soil thickness, and soil permeability. A dynamic cone penetration test was done to determine the thickness of the soil in the research area. For the permeability of the soil in-situ permeability test was done in the study area. Disturbed soil sampling was collected due to the impossibility of undisturbed sampling in the field due to lack of instruments and difficulty in the slope area. An overall field survey was conducted to determine the area of the failure, and soil thickness of the soil.

Laboratory Work

A series of laboratory work was performed to obtain definitive information on the soil properties. The unified Soil Classification System was used to classify the soil after the laboratory tests for porosity, moisture content, unit weight, and so on. The coarse soil particle greater than 2mm was analyzed by using the wet sieve analysis method.

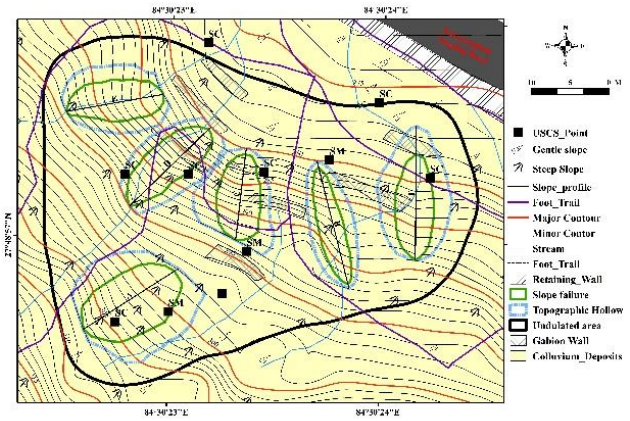

Figure 3, Engineering geological map of the study area.

Table 1, Laboratory Tests with the Standard used in the research work.

Laboratory Tests	Standards
Moisture Content Test	ASTM D2216
Specific Gravity Test	ASTM D854
Atterberg Limit Test	ASTM D4318
Particle Size Distribution	ASTM C136
Direct Shear Test	ASTM 3080
USCS	ASTM D2487

Properties of Slope Materials

The results show that the majority of soil collected from the study area is silty sand and gravel. Based on the grain size analysis of the 14 locations samples, most of them are silty sand (SM) clayey sand (SC). The most common is silty sand.

Figure 4, Process of infiltration test done at the study area.

The ASTM D2487 standard was used to classify the soils in the laboratory. The moisture content of the soil samples varies from 4.65% to 18.27%. The minimum specific gravity of the soil sample is calculated as 2.60

and the maximum specific gravity calculated as 2.79. The minimum and maximum values of infiltration rate obtained from the field work was 6.73E-05 m/sec to 3.71E-04 m/sec. The soil passes from ASTM standard sieve size 2mm was used for the direct shear test. The friction angle of the soils ranges from 26.62° to 39.97° whereas cohesion ranges from 0.08 to 0.26 Kpa.

Figure 5, Showing the process of the sieve analysis.

Slope Characteristics

Based on the flow direction map of the study area slopes were chosen for the modeling and evaluation of the stability of the area. The flow direction map shows the most unstable area on the flow line of the subsurface water in the naturally undulated slope. The most critical part of the slopes was chosen which represents the entire geometry of the study area.

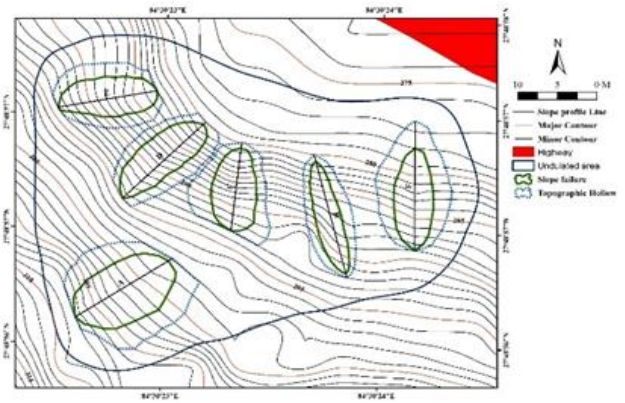

Figure 6, Naturally undulated slope with six failures.

The slope was a natural slope with average slope angles ranging from 31 to 62 degrees. The required geotechnical parameters for modeling were obtained from both field tests and laboratory tests. The slope profile was extracted with the help of Arc Map 10.8, Google Earth Pro, and DEM of the area. In the research area, six slope failures were studied. Named as A, B, C, D, E, and F as indicated in Figure 4. All slope failures were facing toward the northeast direction, recognized in the topographic map using the flow direction map Figure 5. For the seepage and slope stability analysis, all six failure slopes of the naturally undulated slope were chosen for further work.

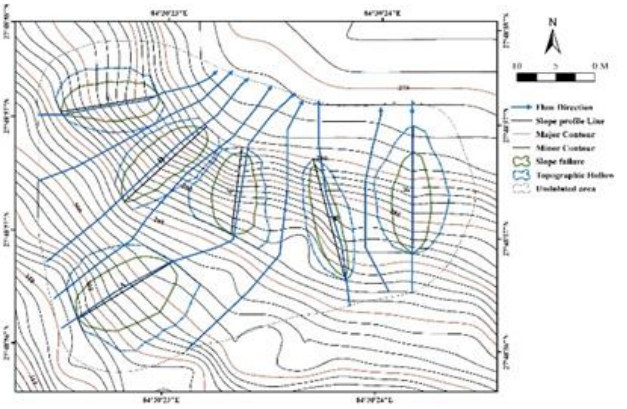

Figure 7, Flow direction map of the research area.

Results

Naturally undulated slopes were a three-dimensional feature of the geomorphological unit. Depth of soil. Length, width, curvatures of profiles i.e. concave (hollow), convex (nose), and straight and plan shapes (convergent, parallel and divergent) represents the hydro-mechanical phenomena occurring in the slope were three-dimensional in nature Dietrich (1987). Slope inclination of the naturally undulated slope was represented by the three-dimensional geometry. To model the hydrologic response of slope in relation with rainfall different models like Hydrological-Stability Model (InH-SM) VanderKwaak (1999) and GEOFS Rigon et al. (2006) were used in the past times.

High quality of data with solutions of large equations were required to solve these stability problems Paniconi et al. (2003). Specification and evaluation of parameters were very difficult in these Hilberts programs (2006). Therefore, the development of two-dimensional program was done for the studying the mechanism of failure of slope during the action of extreme rainfall Carrivick (2007) by reducing the assumptions Lanni (2012). To observe the hydro-mechanical phenomenon for the rainfall induced slope failure in naturally undulated slope two-dimensional approaches were used. The following assumptions were made to apply the two-dimensional approach and get simulations:

- Slope materials fail in a single layer.
- The mode of failure is circular.
- The thickness of soil depth is equal to the maximum depth of failure.
- There are no hydrological relations between colluvium and the bed rock. So that the soil mass was assumed to be impervious.
- The failed slope material is homogeneous and isotropic.
- For both saturated and unsaturated conditions, the hydro-mechanical properties of soils are considered too same for failed mass.

- Rainwater infiltration is assumed to be in transient state conditions.
- The permeability of the soil is equal to the maximum rate of infiltration of soil.

Coupled SEEP/W-SLOPE/W models were frequently used by different researchers to estimate and observe the discharge of the hillslope seepage and capability of the failure during rainfall Dahal et al.(2009). The finite-elements based program SEEP/W in GeoStudio (2018) simulates the distribution of porewater pressure in natural slope whereas SLOPE/W allows limit equilibrium environment for slope. Due to the lack of hydrological model of porewater pressure in SLOPE/W, the modelled information from SEEP/W was directly imported into the SLOPE/W.

Seepage Modelling

For seepage and slope stability modelling, the direction of maximum subsurface flow using DEM of the study area was used to create longitudinal profile of the slopes and soil thickness based on topography of the slope. All profiles were meshed into a fine square element. Soil water characteristic curve (SWCC) function and soil permeability curve (SPC) function were utilized as the input parameters for the modelling. The GeoStudio (2018) environment consists of SWCC function Figure 6 was used for soil with similar gain size distribution pattern whereas Fredlund and Xing (1994) was used to predict the SPC function Figure 7. These two functions were integrated with saturated moisture content and soil permeability field values.

A null flux boundary was assigned for the left vertical edge and the edge below the water table to protect seepage from upper slope section and bedrock. A null flux boundary of the right vertical edge above the water table was specified as potential seepage face. The rain gauge station of Devghat station was utilized as the transient flux to the nodes on the exposed slopping surface with potential seepage face as the upper boundary conditions Figure 8. The relationship of the hillslope hydrology with naturally undulated slopes of the area along the slope profile was simulated by recording the maximum porewater pressure in an area.

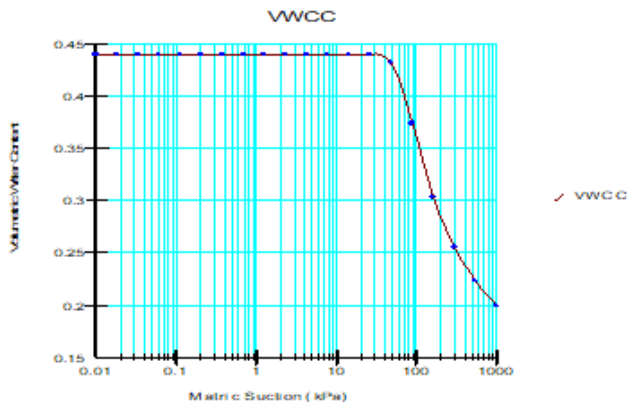

Figure 8, SWCC function used in seepage modelling.

Slope Stability Modelling

The output of the SEEP/W which was two-dimensional seepage simulated is directly linked to SLOPE/W for the stability assessment of the slope. The shear strength due to the role of suction (Φ) was assumed to be two third of Φ'. The presence of organic matter plays a crucial role in decreasing the effective cohesion, effective angle of shearing resistance, and unit weight of the soil Dahal et al. (2011). The calculation of the factor of safety was done by the sensitivity analysis which determines the interrelationship of different parameters as effective cohesion, effective angle of shearing resistance, unit weight, and Φb used in analysis. The minimum and maximum values of effective cohesion, effective angle of shearing resistance, unit weight, and Φ were depends upon the material properties and assigned in the SLOPE/W. To find the slip center and potential failure zone the entry and exit function was assigned. A limit equilibrium analysis was specified by the numbers of iteration. The sliding was divided into vertical slices to reduce the basic equation of the limit equilibrium method. The most critical value was specified by slip surfaces in the simulations.

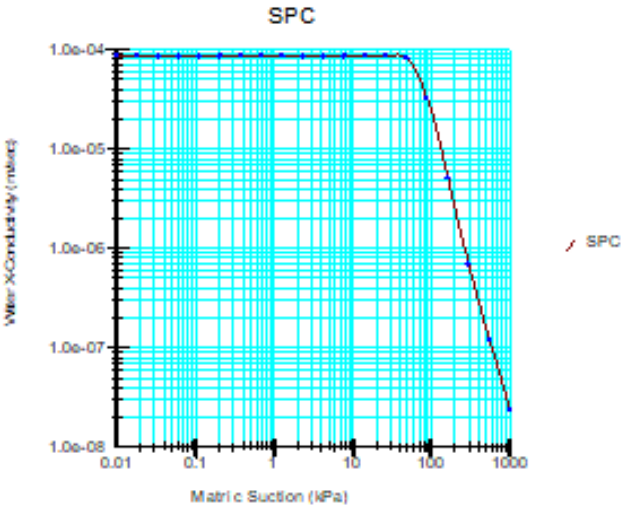

Figure 9, SPC function utilized in seepage modelling.

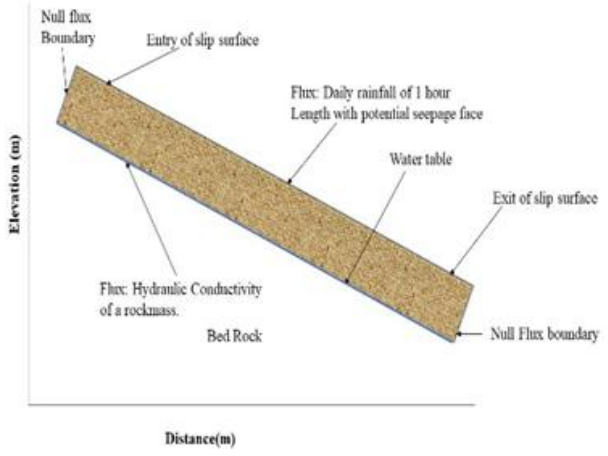

Figure 10, The finite element model used in the research work.

Seepage and Slope Stability analysis

The coupled seepage and slope stability modeling for all six failed slopes were prepared with the help of the flow direction map using the digital elevation model (DEM) of the study area. For the soil thickness data, a topographic break point in the slopes was chosen. All profile sequences were discretized into the mesh of triangle elements of 0.25m. The number of nodes was 223, 216, 164, 208, 144, and 143, whereas the number of mesh elements was 295, 297, 236, 291, 214, and 216 for slope profiles A, B, C, D, E, and F, respectively. The main input parameters used were the soil water characteristic curve (SWCC) function and the soil permeability curve (SPC) function. The slope was simulated using the maximum accumulated rainfall record in 24 hr. at Narayani at Devghat station between 2001 to 2003 A.D. The maximum 24-hour rainfall was discovered in July 31of 2003.

For the slope stability analysis, the seepage simulated in SEEP/W is directly linked to SLOPE/W. The parameters used for modeling are shown in Table 2. To remunerate some uncertainties, sensitivity analysis was performed in stability analysis. Sensitivity analysis helps to examine the interrelation sheep between various parameters used in the analysis and then calculates the factor of safety based on changes in cohesion, angle of shearing resistance, and unit weight. The Morgenstern-Price method with half-sine user-specified interslice force was used to calculate the factor of safety. To find the slip center and the potential failure surface the entry and exit points were used. A limit equilibrium analysis with 2000 iterations was used in each time step.

Table 2, Results of laboratory and field investigations.

Slope Profile Name	Soil Type	L(m)	B(m)	θ(°)	D(m)	C'(KN/m²)	Φ'(°)	γ(KN/m³)	k(m/s)	n
A	SC	13.97	8.36	28.5	0.80-1.10	0.23	28.56	13.91	8.60E-05	0.46
B	SM	17.07	5.48	40	0.65-0.90	0.19	30.62	13.79	7.08E-05	0.45
C	SM	11.91	5.15	44.5	0.47-0.95	0.19	32.97	14.63	1.17E-04	0.44
D	SC	14.7	5.34	44.5	0.43-0.83	0.08	37.7	14.67	8.02E-05	0.43
E	SC	12.64	5.88	43.5	0.45-0.87	0.2	33.08	13.85	7.46E-05	0.44
F	SC	13.63	7.46	35	0.35-0.75	0.23	29.64	14.73	8.62E-05	0.46

Note: In this table, L= slope failure length; B = slope failure breadth; θ= average slope angle; D=Soil thickness; C' = effective cohesion; γ= unit weight of soil; Φ'= effective angle of shearing resistance, K= soil permeability; and n= saturated volumetric water content. C' and Φ' were determined from direct shear test. γ and n were obtained from laboratory experiments. K was measured by field experiment. These values are mean, and therefore a factor of safety via sensitivity computation was performed during slope stability analysis.

For further simulations, different return periods of the 24-hour maximum rainfall of 31 July 2003 were considered. The hydraulic function employed in the previous simulation was used using the 5 years return period of rainfall. The Gumbell technique was used to compute the return period. The variation of porewater pressure with the topographic hollow area is shown in Figure 9 for a 5-year return period. Using the area of the topographic hollow and the maximum porewater pressure data recorded, a threshold relation between the maximum porewater pressure and the topographic hollow area was established in Figure 10. The threshold equation by using the maximum porewater pressure with the topographic hollow area for the 5-year return period of rainfall expressed as

$$u = 0.0564 \times a0.9956$$

where u is the maximum porewater pressure in Kpa and a is the area of topographic hollow in sq. m.

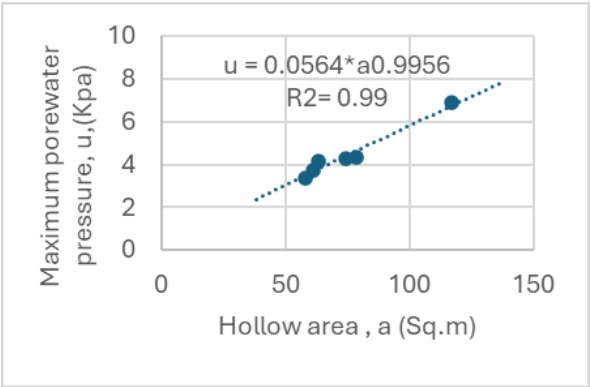

Figure 11, Variation of maximum porewater pressure with topographic hollow area for 5-year return period.

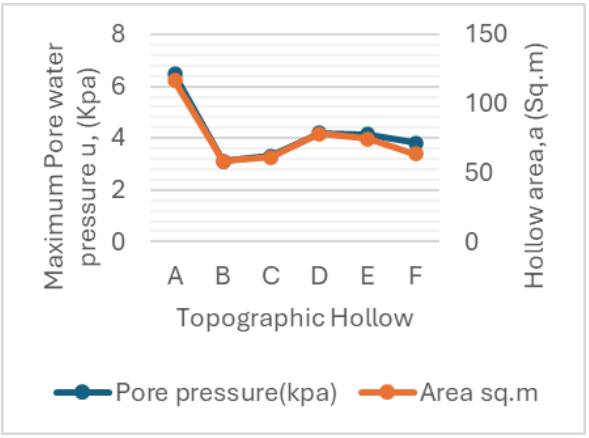

Figure 12, Porewater pressure and topographic hollow area threshold cure for slope failures for 5-year return period.

Table 3, Maximum Porewater pressure- topographic hollow area threshold equations for slope failure for different period of time.

Time	Threshold equation
24 hrs max	$u = 0.09*a^{0.9413}$
5-year return	$u = 0.0564*a^{0.9956}$
10-year return	$u = 0.0768*a^{0.9398}$
25-year return	$u= 0.092*a^{0.9063}$
50-year return	$u = 0.0985*a^{0.9029}$
100-year return	$u = 0.1279*a^{0.8708}$

The factors of safety calculated by using the 5-year return period rainfall data were 0.494, 0.889, 0.380, 0.694, 0.457, and 0.359 respectively for the slopes A, B, C, D, E, and F. The factor of safety values shows that slopes were in very critical condition. The optimized critical slip surfaces and respective factors of safety for all slopes.

The empirical relation between the maximum discharge of hillslope seepage and the topographic hollow area presented in this study for 24 hrs maximum rainfall data and their 5, 10, 25, 50, and 100 years return period.

Discussion

In past studies in the context of Nepal, the problem caused by the discharge of hillslopes and slope instability in naturally undulated slopes was not studied in detail. This study mainly focused on topographic hollows present in the naturally undulated slope and explicitly presented the hydrological and mechanical phenomenon in hollows responsible for the development of slope failure during a heavy rainfall event. The role of topographic hollows on hill slope hydrology and slope stability can be understood when they are recognized. In this research, six topographic hollows A, B, C, D, E, and F were identified in the digital elevation model based on flow direction characteristics. All the hollows in the study area were elliptical. The maximum porewater pressure developed in the topographic hollows were 7.84, 3.95, 4.43, 5.49, 5.34, and 4.5 kPa for A, B, C, D, E, and F respectively by using 24-hour maximum rainfall data. The bigger the size of hollows it produces the higher porewater pressure leads to the higher amount of subsurface follow and vice versa.

An equation of threshold relationship representing maximum porewater pressure and the hollow area was established for the 24 hrs. maximum rainfall with their return period of 5, 10, 25, 50, and 100 years as represented in Table 3 and their porewater pressure variation was shown in Figure 11. Slope failures A, B, C, D, E, and F were identified in the hollows. All these slope failures were caused by the rainfall event. So, the maximum rainfall of 2001 to 2023 years was analyzed and 24 hrs maximum rainfall was used for the simulation. Thus, the seepage and slope stability simulations were performed for the six slopes using GeoStudio 2018 to understand the hydrological and stability conditions of the topographic hollows present in the naturally undulated slopes. In the seepage modeling, transient positive and negative pore pressure was noted in all nodes in the direction of potential slip faces during rainfall events. The discharge of hillslope seepage and instability in the topographic hollows are three-dimensional but these were researched by using two-dimensional observation in this research. The finite element mesh model of slope failure profiles was used in numerical modeling using parameters like soil thickness, slope gradient, and slope length. These are the basic topographic parameters of slope mass triggering as they are used to determine the initial subsurface zone storage before rainfall. The result and finding of this two-dimensional modeling in this research should not deviate from the actual hydro-mechanical phenomenon in the topographic hollows. The empirical relation between the maximum discharge of hillslope seepage and the topographic hollow area presented in this study for 24 hrs maximum rainfall data and their 5, 10, 25, 50, and 100 years return period. These relationships are thought to help improve the understanding of the development of the discharge of hillslope seepage in hollows. Knowing about the accuracy of the empirical parameters relationship to predict the discharge of hillslope seepage, further research is needed. Hence, similar types of work should be repeated in others catchment of related geophysical settings.

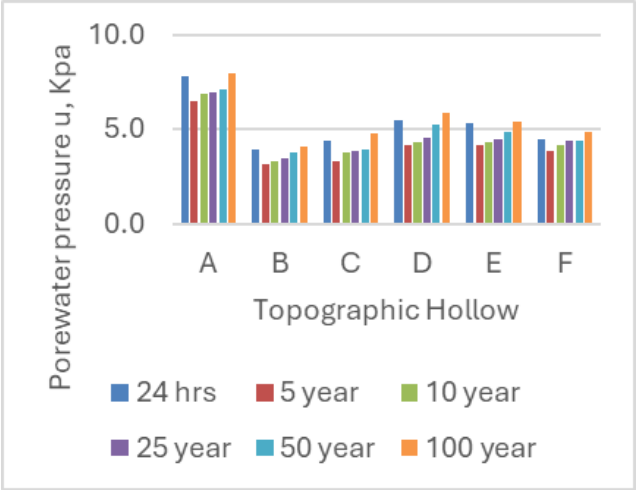

Figure 13, Histogram shows porewater pressure develop at hollow at different period of time comparison.

Conclusion

A series of fully coupled hydro-mechanical simulations were conducted to evaluate the development of positive and negative pore water pressures and their effect on the factor of safety (FoS) of a naturally undulated slope. The time-dependent analysis revealed that rapid removal of stress leads to the development of higher negative excess pore water pressure (suction), which in turn results in temporarily elevated FoS values. The water table was found to be a critical factor in pore pressure dynamics: below the water table, pore pressure is positive; above it, soils remain saturated due to capillary rise but exhibit negative pore pressures (matric suction), influencing slope stability.

Geologically, the study area is located within the Labdi Member of the Nourpul Formation, predominantly composed of phyllite. Engineering geological mapping identified features such as minor landslides, gully erosion, and shallow slope failures. Data from the Narayani (Devghat) rainfall station confirmed that the area receives intense and prolonged monsoonal

rainfall, with extreme 24-hour events, particularly in 2003, contributing to elevated failure risks.

Key findings indicate that slope failure is closely linked to the interplay between rainfall intensity and duration, pore water pressure distribution, and slope geometry. Long-duration rainfall events were observed to cause a significant increase in pore water pressure, reducing matric suction and weakening slope materials. In contrast, short-duration events had comparatively minor effects.

Finite element seepage analyses using both saturated and unsaturated flow conditions provided critical insights into temporal variations in pore water pressure, volumetric water content, and total hydraulic head. These simulations confirmed that larger naturally undulated slopes exhibit greater hillslope seepage, with the highest pore pressures developing in lower elevation hollows.

Overall, the study concludes that hydrological conditions, rainfall characteristics, and slope geometry are dominant factors controlling rainfall-induced slope failures. Effective seepage management and early warning systems are recommended to mitigate future hazards in similar geomorphic settings.

References

Acharya, K. P., Bhandary, N. P., Dahal, R. K., and Yatabe, R. (2016). Seepage and slope stability modelling of rainfall-induced slope failures in topographic hollows. Geomatics, Natural Hazards and Risk, 7(2), 721-746. https://doi.org/10.1080/19475705.2014.954150

Acharya, K. P., Yatabe, R., Bhandary, N. P., and Dahal, R. K. (2016). Deterministic slope failure hazard assessment in a model catchment and its replication in neighbourhood terrain. Geomatics, Natural Hazards and Risk, 7(1), 156-185. http://dx.doi.org/10.1080/19475705.2014.880856

Amatya, K., and Jnawali, B. (1994). Geological map of Nepal, scale: 1: 1,000,000. Department of mines and geology, International centre for integrated mountain development, Carl Duisberg Gesellschaft e. V., and United Nations environment programme.

Arita, K. (1973). Kathmandu region. Geology of the Nepal Himalayas, 99-145.

Auden, J. (1935). Traverses in the Himalaya. Records of Geological survey of India, 69, 123-167.

Beven, K. J., and Kirkby, M. J. (1979). A physically based, variable contributing area model of basin hydrology/Un modèle à base physique de zone d'appel variable de l'hydrologie du bassin versant. Hydrological sciences journal, 24(1), 43-69. https://doi.org/10.1080/02626667909491834

Bordet, P., Remy, M., Krummenacher, D., and R, M. (1964). Sur la stratigraphie des séries affleurant dans la vallée de la Kali Gandaki (Nepal central). Comptes Rendus Hebdomadaires Des Seances De L Academie Des Sciences, 259(2), 414-and.

Bronstert, A. (1994). Modellierung der Abflussbildung und der Bodenwasserdynamik von Hangen Dissertation, Karlsruhe, Karlsruher Institut für Technologie (KIT), 1994].

Campbell, R. H. (1975). Soil slips, debris flows, and rainstorms in the Santa Monica Mountains and vicinity, southern California (Vol. 851). US Government Printing Office. https://doi.org/10.3133/pp851

Cardinali, M., Galli, M., Guzzetti, F., Ardizzone, F., Reichenbach, P., and Bartoccini, P. (2006). Rainfall induced landslides in December 2004 in south-western Umbria, central Italy: types, extent, damage and risk assessment. Natural Hazards and Earth System Sciences, 6(2), 237-260. https://doi.org/10.5194/nhess-6-237-2006.

Carrivick, J. L. (2007). Hydrodynamics and geomorphic work of jökulhlaups (glacial outburst floods) from Kverkfjöll volcano, Iceland. Hydrological Processes: An International Journal, 21(6), 725-740. http://dx.doi.org/10.1002/hyp.6248

Crosta, G. (1998). Regionalization of rainfall thresholds: an aid to landslide hazard evaluation. Environmental Geology, 35(2-3), 131-145. https://doi.org/10.1007/s002540050300

Crozier, M. J. (1999). Prediction of rainfall-triggered landslides: A test of the antecedent water status model. Earth Surface Processes and Landforms: The Journal of the British Geomorphological Research Group, 24(9), 825-833. https://doi.org/10.1002/(sici)1096-9837(199908)24

Dahal, R. K., and Hasegawa, S. (2008). Representative rainfall thresholds for landslides in the Nepal Himalaya. Geomorphology, 100(3-4), 429-443. https://doi.org/10.1016/j.geomorph.2008.01.014

Dahal, R. K., Hasegawa, S., Nonomura, A., Yamanaka, M., Masuda, T., and Nishino, K. (2008). GIS-based weights-of-evidence modelling of rainfall-induced landslides in small catchments for landslide susceptibility mapping. Environmental Geology, 54, 311-324. http://dx.doi.org/10.1007/s00254-007-0818-3

Dahal, R. K., Hasegawa, S., Yamanaka, M., and Bhandary, N. P. (2011). Rainfall-induced landslides in the residual soil of andesitic terrain, western Japan. Journal of Nepal Geological Society, 42, 137-152. https://doi.org/10.3126/jngs.v42i0.31461

Dahal, R. K., Hasegawa, S., Yamanaka, M., Dhakal, S., Bhandary, N. P., and Yatabe, R. (2009). Comparative analysis of contributing parameters for rainfall-triggered landslides in the Lesser Himalaya of Nepal. Environmental Geology, 58, 567-586. http://dx.doi.org/10.1007/s00254-008-1531-6

Dhital, M. R. (2015). Geology of the Nepal Himalaya: regional perspective of the classic collided orogen. Springer. http://dx.doi.org/10.1007/978-3-319-02496-7

Dietrich, W. (1987). Overview:" Zero-order basins" and problems of drainage density, sediment transport and hillslope morphology. International Association of Hydrological Sciences Publication, 165, 27-37.

Dietrich, W., and Dunne, T. (1978). Sediment budget for a small catchment in a mountainous terrain. http://dx.doi.org/10.1130/0091-7613(2001)029

Dietrich, W. E., de Asua, R. R., Coyle, J., Orr, B., and Trso, M. (1998). A validation study of the shallow slope stability model, SHALSTAB, in forested lands of Northern California. Stillwater Ecosystem, Watershed and Riverine Sciences. Berkeley, CA.

Dunne, T. (1978). Field studies of hillslope flow processes. Hillslope hydrology, 227-293.

ESCAP, U. (1993). Cambodia. United Nations.

Frattini, P., Crosta, G., and Sosio, R. (2009). Approaches for defining thresholds and return periods for rainfall-triggered shallow landslides. Hydrological Processes: An International Journal, 23(10), 1444-1460. https://doi.org/10.1002/hyp.7269

Fredlund, D. G., and Xing, A. (1994). Equations for the soil-water characteristic curve. Canadian geotechnical journal, 31(4), 521-532. https://doi.org/10.1139/t94-061

Gansser, A. (1964). Geology of the Himalayas Interscience Publishers London. UK New York, NY, USA Sydney, Australia.

Guzzetti, F., Cardinali, M., Reichenbach, P., Cipolla, F., Sebastiani, C., Galli, M., and Salvati, P. (2004). Landslides triggered by the 23 November 2000 rainfall event in the Imperia Province, Western Liguria, Italy. Engineering Geology, 73(3-4), 229-245. https://doi.org/10.1016/j.enggeo.2004.01.006

Hagen, T. (1969). Geology of Nepal Himalaya. Report on the geological Survey of Nepal Preliminary Reconnaissance. Zurich. Memoires de la Soc. Helvetique des science Naturelles, 86, 185.

Hagen, T. (1969). Report on the geological survey of Nepal. Denkschr. Schweiz. Naturf. Ges., 81, 185.

Hilberts, A. G. J. (2006). Low-dimensional modeling of hillslope sub-surface flow processes: developing and testing the hillslope-storage Boussinesq model. Wageningen University and Research. https://doi.org/10.1029/2006WR004964

Jacob, A., Thomas, A. A., Nath, A. G., and MP, A. (2018). Slope stability analysis using Plaxis 2D. International Research Journal of Engineering and Technology (IRJET), 5(4), 3666-3668.

Janbu, N. (1973). Slope stability computations. Publication of: Wiley (John) and Sons, Incorporated.

Khan, M. I., and Wang, S. (2021). Slope stability analysis to correlate shear strength with slope angle and shear stress by considering saturated and unsaturated seismic conditions. Applied Sciences, 11(10), 4568. http://dx.doi.org/10.3390/app11104568

Kvalstad, T. J., Nadim, F., Kaynia, A. M., Mokkelbost, K. H., and Bryn, P. (2005). Soil conditions and slope stability in the Ormen Lange area. Marine and Petroleum Geology, 22(1-2), 299-310. http://dx.doi.org/10.1016/j.marpetgeo.2004.10.021

Lanni, C. (2012). Hydrological controls on the triggering of shallow landslides: from local to landscape scale University of Trento].

Le Fort, P. (1975). Himalayas: the collided range. Present knowledge of the continental arc. American Journal of Science, 275(1), 1-44.

Marquez, R. M. (2004). Three-dimensional slope stability analysis using finite elements. 2000-2009-Mines Theses and Dissertations.

Pack, R. T., Tarboton, D. G., and Goodwin, C. (1999). SINMAP 2.0-A stability index approach to terrain stability hazard mapping, user's manual.

Paniconi, C., Troch, P. A., van Loon, E. E., and Hilberts, A. G. (2003). Hillslope-storage Boussinesq model for subsurface flow and variable source areas along complex hillslopes: 2. Intercomparison with a three-dimensional Richards equation model. Water resources research, 39(11). http://dx.doi.org/10.1029/2002WR001728

Pasuto, A., and Silvano, S. (1998). Rainfall as a trigger of shallow mass movements. A case study in the Dolomites, Italy. Environmental Geology, 35(2-3), 184-189.

Paudyal, K. (2017). Geological and Petrological evolution of the Lesser Himalaya between Mugling and Damauli, central Nepal

Paudyal, K., Adhikari, L., Maharjan, N., and Paudel, L. (2012). Geological setting and lithostratigraphy of Bandipur-Gondrang area of Lesser Himalaya, central Nepal. Bulletin of the Department of Geology, 15, 49-62. https://doi.org/10.3126/bdg.v15i0.7417

Paudyal, K., and Paudel, L. (2011). Geological setting and lithostratigraphy of the Lesser Himalaya in the Mugling-Banspani area, central Nepal. Journal of Nepal Geological Society, 42, 51-63. https://doi.org/10.3126/jngs.v42i0.31449

Pradhan, S. (2014). Stability analysis of open PIT slope using FLAC

Rigon, R., Bertoldi, G., and Over, T. M. (2006). GEOtop: A distributed hydrological model with coupled water and energy budgets. Journal of Hydrometeorology, 7(3), 371-388. https://doi.org/10.1175/JHM497.1

Sassa, K. (1986). The mechanism of debris flows and the forest effect on their prevention. 18th IUFRO World Congress, Ljubljana, Yugoslavia, IUFRO.

Setyawan, A., Alina, A., Suprapto, D., Gernowo, R., Suseno, J. E., and Hadiyanto, H. (2021). Analysis slope stability based on physical properties in Cepoko Village, Indonesia. Cogent Engineering, 8(1), 1940637. https://doi.org/10.1080/23311916.2021.1940637

Shrestha, S., Shrestha, J., and Sharma, S. (1984). Geological Map of Eastern Nepal, 1: 250 000. Ministry of Industry, Department of Mines and Geology, Lainchour, Kathmandu.

Sidle, R. (1987). A dynamic model of slope stability in zero order basin. IAHS publ., 165, 101-110.

Stöcklin, J. (1980). Geology of Nepal and its regional frame: Thirty-third William Smith Lecture. Journal of the Geological Society, 137(1), 1-34. https://doi.org/10.1144/gsjgs.137.1.0001

Stöcklin, J., and Bhattarai, K. (1977). Geology of Kathmandu area and Central Mahabharat range: Nepal Himalaya.

Sun, Y., Yang, K., Hu, R., Wang, G., and Lv, J. (2022). Model Test and Numerical Simulation of Slope Instability Process Induced by Rainfall. Water, 14(24), 3997. https://doi.org/10.3390/w14243997

Tater, J., Shrestha, S., Shrestha, J., and Sharma, S. (1983). Geological map of western central Nepal, scale 1: 250,000. Department of Mines and Geology, Kathmandu.

Tsukamoto, Y., and Minematsu, H. (1987). Hydrogeomorphological characteristics of a zero-order basin. IAHS-AISH publication (165), 61-70.

Van Asch, T. W., Buma, J., and Van Beek, L. (1999). A view on some hydrological triggering systems in landslides. Geomorphology, 30(1-2), 25-32. https://doi.org/10.1016/S0169-555X(99)00042-2

VanderKwaak, J. E. (1999). Numerical simulation of flow and chemical transport in integrated surface-subsurface hydrologic systems.

Wagner, A., Leite, E., and Oliver, R. (1990). A landslide hazard mapping software (version 1.0), 2 volumes. ITECO CH and University of Lausanne, Switzerland, 4.